The Prediction of Fracture Toughness from Specific Microstructural Measurements in Engineering Alloys

P.F. Timmins

This paper reports on an investigation based on sharp-crack and blunt-notch toughness and microstructural measurements whereby toughness values are predicted from measuring the microstructural feature that dominates toughness. Three engineering alloys are investigated: pearlitic ductile iron, rail steel, and Zircodyne 7 (Zr-Nb). Examples of toughness prediction in engineering applications are presented in terms of specific microstructural measurements and phases dominating toughness and in terms of selecting and specifying alloys to meet service conditions.

Keywords
fracture toughness, microstructure, void size

1. Introduction

MACROSCOPIC plane-strain elastic fracture toughness, K_{Ic}, and macroscopic plane-strain elastic-plastic crack growth toughnesses (Ref 1) are controlled by microscopic separation events that take place on a microstructural size scale (Ref 2). The notion that these events are governed by a "characteristic distance" in the microstructure is probably true (Ref 3), but only in the sense that this "distance" characterizes a specific microstructural feature that dominates the microstructure insofar as it governs the macroscopic toughness parameter. This paper describes specific microstructures in three different commercial alloys and demonstrates the potency of the "dominant" microstructural feature, in each case, in predicting toughness in sharp-cracked and blunt-notched tests.

2. Experiment

Details of the test procedures have already been reported (Ref 1, 4, 7). Tests were performed on commercial grades of various compositions of pearlitic ductile iron, commercial-grade rail steel of near-eutectoid composition, and commercial-grade Zircodyne 7 (Teledyne Wah-Chang, Albany, Oregon) (Zr-Nb); the compositions are shown in Table 1.

P.F. Timmins, President, Risk Based Inspection Inc., 2233 Timberlane Dr., Abbotsford, BC, V3G 1E4, Canada

3. Results

3.1 *Pearlitic Ductile Iron*

In an early investigation into the effect of microstructural variables on the elastic fracture toughness of pearlitic ductile cast irons, Holdsworth and Jolley (Ref 4) reported values of K_{Ic} for several such irons. Their K_{Ic} values, together with their microstructural information on the spheroidal graphite nodules/mm^2 for the five irons investigated, are shown in Table 2. The pearlitic irons were produced by air cooling after holding for 6 h at 1173 K.

The toughness results were obtained on fatigue precracked specimens 10 mm thick and 20 mm wide, loaded in three-point bending. The pearlitic ductile irons gave valid K_{Ic} data at 298 K, as defined in ASTM E 399. The method of measuring the area fraction of graphite nodules was not described, but presumably a standard metallographic technique was employed.

The validity of the Holdsworth and Jolley data, presented as Fig. 1 in the present work, is in the linear nature of the relationship between the number of nodules/mm^2 and the elastic fracture toughness at 298 K. That is, the feature in the microstructure that has the greatest influence on the toughness is the area fraction of graphite nodules, rather than, say, the interlamella spacing of the pearlite. This concept of the predomi-

Table 1 Compositions of alloys

Iron	Composition, %							
	C	Si	Mn	S	P	Ni	Mg	Inoculant
Pearlitic Ductile Irons (Ref 4)								
1	3.64	2.38	3.35	0.016	0.024	0.88	0.072	¼%Fe/Si
2	3.62	2.41	0.34	0.016	0.024	0.83	0.064	½%Fe/Si + Bi
3	3.63	2.42	0.32	0.016	0.024	0.083	0.010	½%Fe/Si
4	2.58	2.16	0.45	0.020	0.025	0.081	0.054	½%Fe/Si
5	3.99	2.34	0.39	0.014	0.025	0.88	0.078	½%Fe/Si
Rail steels								
Nominally 0.85 wt% C								
Zircodyne 7 (Zr-Nb)								
Nominally Zr-2.5wt% Nb								

nant feature in the microstructure and the influence it has on toughness was introduced by Firrao (Ref 5) and later illustrated to be applicable to at least one other system, the Zr-2.5wt% Nb alloy Zircodyne 7 (Ref 1).

3.2 *Rail Steel*

The dynamic lower-shelf Charpy impact toughness of rail steels of various MnS inclusion levels and various interlamella pearlite spacings was investigated at 233 K (Ref 7). The lower-shelf level was found to be independent of nonmetallic inclusion content but dependent on the interlamella spacing of the pearlite in these steels of nominal eutectoid composition.

The available data show the dependence of microhardness on pearlite spacing. Figure 2 reflects the lower-shelf toughness dependence in rail steels (Ref 7), that is, the absolute level of the lower-shelf increases with decreasing spacing of the pearlite.

3.3 *Zircodyne 7*

The elastic-plastic fracture toughness of Zircodyne 7 (Zr-Nb) was investigated at 298 K, and J-resistance curves were produced in accord with ASTM E 813, using 17 mm compacts in the following heat-treated conditions (Ref 1):

- 30% cold work + 24 h at 673 K, fast cool—"as-received" condition
- Furnace cooled after 30 min at 1123 K
- Water quenched after 10 min at 1273 K + 24 h at 773 K, furnace cooled
- Water quenched after 10 min at 1143 K + 24 h at 773 K, furnace cooled

The microstructures resulting from the four heat-treated conditions investigated were in accord with those reported in a review by Northwood and Lim (Ref 6). That is, the morphology of the $\alpha + \beta$ phases was altered by heat treatment, particularly in the furnace-cooled specimens and the quenched and aged specimens, but the dominant microstructural effect was the size and distribution of the zirconium hydrides, which was also greatest in the furnace-cooled and the quenched and aged specimens.

Sections were cut through the regions of stable crack growth such that the crack profiles could be examined. For each of the four heat-treated conditions, an attempt was made to relate the microstructures to features observed on the fracture surfaces. The section through the stable crack growth region for the furnace-cooled specimen and the corresponding fracture surface are shown in Fig. 3. The similar sections for the specimen quenched from 1143 K and aged at 773 K are shown in Fig. 4. The hydrides formed during heat treatment dominated these microstructures and played a key role in the ductile fracture of the specimens.

Table 2 Toughness/area fraction of spheroidal graphite for pearlitic ductile irons

K_{Ic}, MPa$\sqrt{m}$	Graphite nodules/mm^2	Iron number(a)
30.5	20.6	4
31.5	37.2	1
32	52.4	3
33.5	73.8	5
34.75	106.8	2

(a) From Table 1

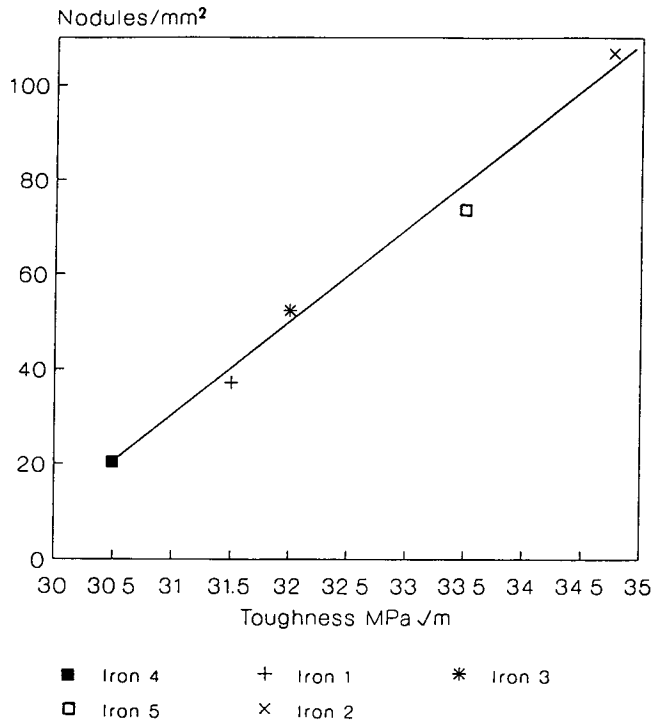

Fig. 1 Effect of area fraction of graphite nodules on toughness of ductile iron that was air cooled at 1173 K

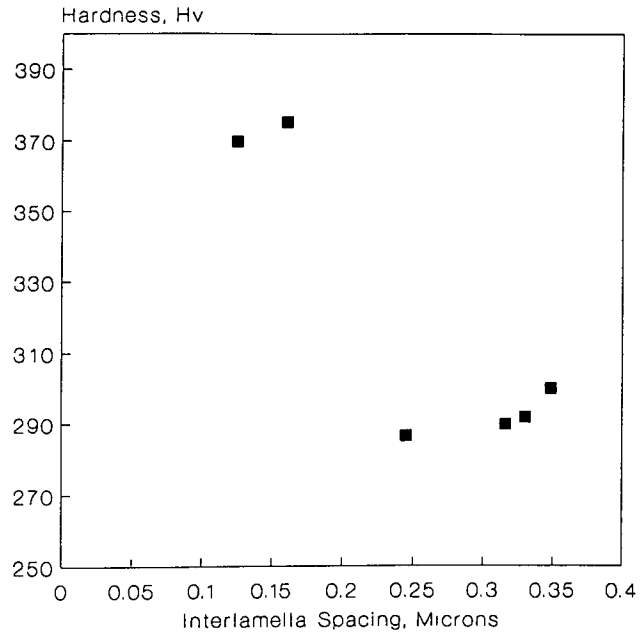

Fig. 2 Change in hardness with interlamella spacing of pearlite in rail steels

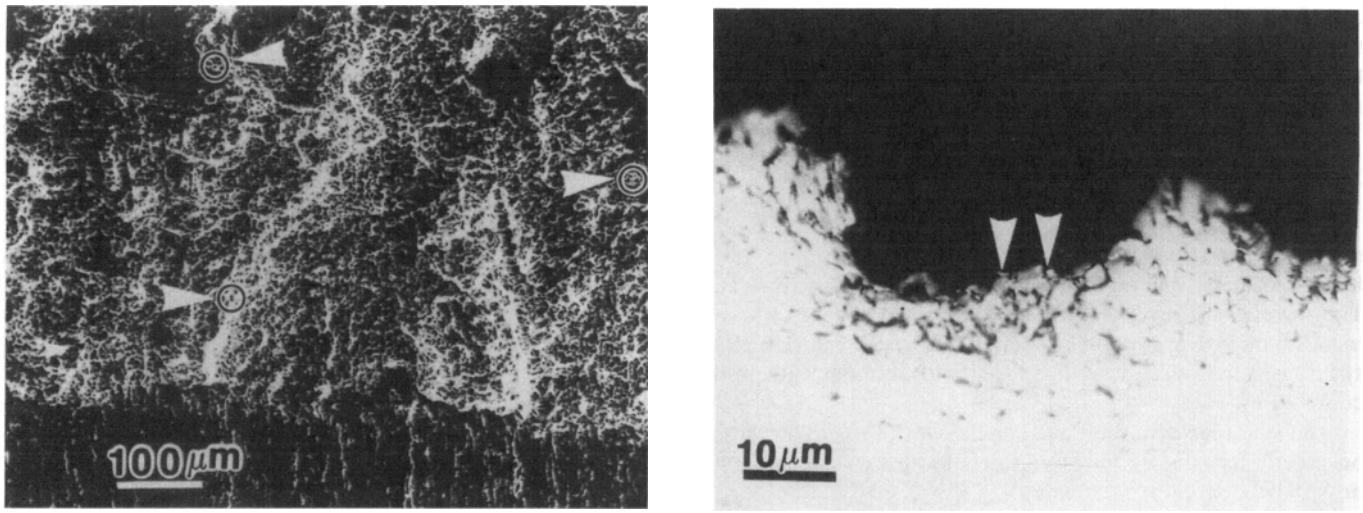

(a) (b)

Fig. 3 (a) Scanning electron micrograph showing ductile fracture. The arrowed circles enclose approximately three major voids to give a major void size of 12 μm. (b) Optical micrograph of a section cut through the stable crack growth region. The arrows indicate intergranular hydrides, the dominant microstructural feature causing the major voids. The hydride filaments are about 12 μm long.

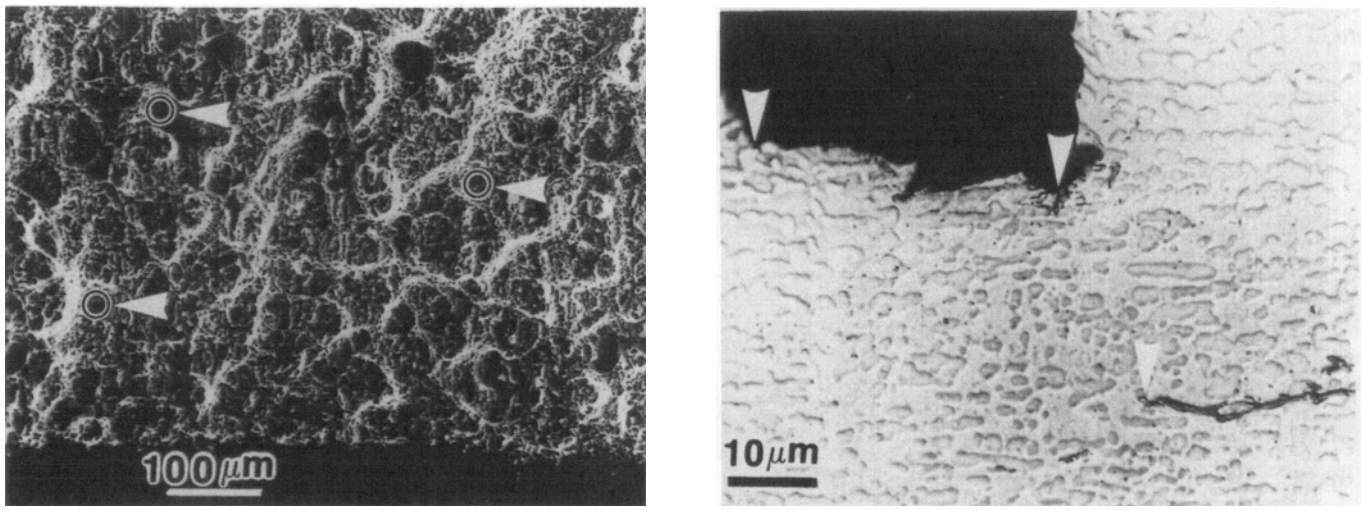

(a) (b)

Fig. 4 (a) Scanning electron micrograph showing ductile fracture. The arrowed circles are of the same diameter as the major voids, approximately 36 μm. (b) Optical micrograph of a section cut through the stable crack growth region. The arrows indicate massive hydrides and a sheared-out hydride interface, the dominant microstructural feature causing the major voids. The hydride filaments are about 36 to 40 μm long.

4. Discussion

The dominant microstructural feature that governs the plane-strain elastic fracture toughness of pearlitic ductile iron is, without a doubt, the area fraction of graphite nodules. This is true irrespective of the precise mechanisms taking place in some "process zone" ahead of the advancing crack tip and irrespective of what some notion of "microscopic" toughness might be (Ref 3). By the same token, the dominant microstructural feature that governs the Charpy blunt-notch lower-shelf toughnesses of rail steels is the interlamella spacing of the pearlite.

Both these microstructures contained large volumes of different phases. The pearlitic ductile iron contained pearlite and nodules of graphite. The near-euctectoid rail steels contained massive MnS stringers and pearlite. For these two materials, which failed in a brittle manner, the "dominant" microstructural features are clearly defined: graphite in the iron and pearlite in the rail steel.

Regarding the elastic-plastic toughness behavior of Zircodyne 7 (Zr-Nb), much attention was paid to the "void diameter" in the experimental approach (Ref 1). Figures 3 and 4 illustrate the need for both SEM and optical microscopy of the fracture surface in deciding which characteristic feature of the

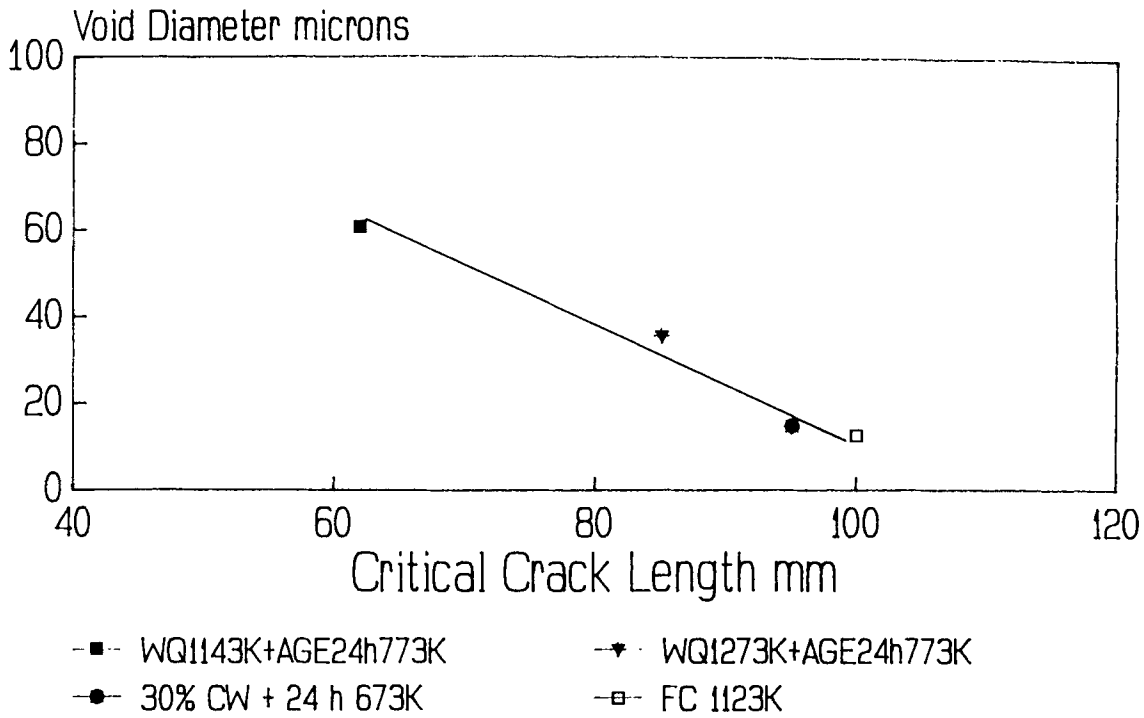

Fig. 5 Effect of mean void diameter on the critical crack length of heat-treated pressure tube

fracture surface and the microstructure gives rise to the void diameter that is appropriate for a given ductile fracture process. In Fig. 3 the appropriate void size is that which corresponds to the finer hydrides that act as void nuclei in this matrix. In Fig. 4, the appropriate void size is that which corresponds to regions of material that have been "sheared out" of the fracture surface as a consequence of easy separation along the massive hydride-matrix interfaces.

This concept of attributing ductile fracture to events involving a "major void diameter" (i.e., that associated with the dominant microstructural feature), proposed by Firrao (Ref 5), is in keeping with the observations and measurements made for defining a microstructural feature that characterizes the ductile fracture mechanism of Zr-Nb subjected to various heat treatments. Clearly the magnitude of the "major void diameter" varies with microstructure. In Fig. 3 the major void diameter is of the order of 12 μm, whereas in Fig. 4 it is of the order of 36 μm. The smaller the value of "major void diameter," the greater the crack growth toughness (Ref 1).

From a predictive capability standpoint, the toughness/dominant microstructural feature relationships have distinct advantages in the areas of design and failure control. In pearlitic ductile iron, consider now the exploitation of the relationship in Fig. 1 in the defect tolerance analysis of, for example, a valve body in a Christmas tree for use on the oil patch. Let the number of graphite nodules/mm^2 be 20, the residual stress in the valve body be 120 MPa, and the proof stress be 550 MPa. From Fig. 1, K_{Ic} is 30.5 MPa$\sqrt{m}$. Determine the tolerable defect size with the aspect ratio of the crack as follows:

$$\frac{a}{2c} = \frac{1}{10}$$

$$\frac{a}{\phi} = \frac{(K_{Ic})^2}{1.21\pi\sigma^2} = \frac{30.5 \times 30.5}{1.21 \times \pi \times 120 \times 120} = 0.01699 \text{ m}$$

From Ref 8:

$$\phi = 1.1$$

$$a = 18.77 \text{ mm}$$

The defect must be more than 18.7 mm deep before fracture would occur. However, the customer has specified that the safe defect size must be greater than 20.0 mm. Thus, from Fig .1, the microstructure giving rise to an increased elastic fracture toughness must be employed. A microstructure containing approximately 70 nodules/mm^2 would give a toughness level of 33 MPa$\sqrt{m}$. As before:

$$\frac{a}{\phi} = \frac{(K_{Ic})^2}{1.21\pi\sigma^2} = \frac{33 \times 33}{1.21 \times \pi \times 120 \times 120} = 0.01989 \text{ m}$$

and

$$\phi = 1.1$$

$$a = 21.88 \text{ mm}$$

Thus, the safe defect size is now 21.88 mm, in keeping with the customer specification of 20.00 mm minimum.

In rail steels, consider what would be specified for the safest rail operating in, for example, a Canadian winter, where temperatures can fall to 233 K (–40 °C). Clearly the rail with the

smallest interlamella spacing of pearlite, say 0.10 μm (from Fig. 2) should be selected.

Finally, by plotting the void diameter associated with the dominant microstructural feature against the critical crack length, a very potent engineering relationship resulted for Zircodyne 7 (Zr-Nb), as shown in Fig. 5. This is the ability to predict the critical crack length of Zr-Nb pressure tubes from a knowledge of the void diameter in the stable crack growth region of 17 mm compact test specimens. Careful control of zirconium hydride size and distribution can give rise to a critical crack length of up to 100 mm in pressure tubes manufactured from this material.

5. Conclusions

- Precise knowledge of the dominant feature in three different alloys of different microstructures yielded the ability to predict fracture toughness.
- Closer control of the failure behavior of components can be imposed if the relationships between microstructure and fracture toughness are defined.
- These relationships appear to be alloy specific, and their definition for a wide range of alloys should appeal to researchers in this field.

Acknowledgments

I am grateful to Ann Timmins, who was responsible for the experimental work on the Zr-Nb and the rail steels. Thanks are also due to Carol Cumpstone, who typed the manuscript.

References

1. P.F. Timmins, "The Influence of Heat Treatment on the Fracture Toughness of Zr-2.5 wt% NB," invited paper, Eighth European Conference on Fracture (Turin, Italy), Oct 1990
2. R.O. Ritchie, J.F. Knott, and J.R. Rice, *J. Mech. Phys. Solids,* Vol 21, 1973, p 395
3. P. Bowen, S.G. Druce, and J.F. Knott, *Acta Metall.,* Vol 35, 1987, p 1735
4. S.R. Holdsworth and G. Jolley, *Source Book on Ductile Iron,* American Society for Metals, 1977, p 305
5. D. Firrao, private communication, March 1989
6. D. Northwood and D. Lim, *Can. Metall. Quart.,* Vol 18, 1979, p 441
7. P.F. Timmins, "Executive Summary of the Clean Steel Program," CN Rail Technical Research Center, June 1987
8. J.M. Svoboda, Research Report 94A, Steel Founder's Society of America, Oct 1982